Spectroscopic Studies of Dehydrogenation of Ammonia Borane in Carbon Cryogel

Saghar Sepehri,[†] Aaron Feaver,[†] Wendy J. Shaw,[‡] Christopher J. Howard,[‡] Qifeng Zhang,[†] Tom Autrey,*[,‡] and Guozhong Cao*[,†]

Materials Science and Engineering, University of Washington, 302 Roberts Hall, Box 352120, Seattle, Washington 98195, and Pacific Northwest National Laboratory, P.O. Box 999, Richland, Washington 99352

Received: September 3, 2007; In Final Form: October 11, 2007

Ammonia borane (AB) is of great interest for storing hydrogen, an important issue in the growing field of hydrogen technology. The reaction pathways leading to the thermal decomposition of solid-state AB incorporated in carbon cryogels (CC) have been studied by spectroscopic methods. The time-dependent thermal decomposition was followed by in situ ^{11}B nuclear magnetic resonance (NMR) and showed a significant increase in hydrogen release kinetics for AB in CC compared to neat AB. Both ^{11}B NMR and Fourier transform infrared spectroscopy show a new reaction product, formed in the thermal decomposition of AB in CC scaffold (CC−AB) that is assigned to reactions with surface oxygen groups. The results indicate that incorporation of AB in CC enhances kinetics because of the reactions with residual surface-bound oxygen functional groups. The formation of new products with surface −O−B bonds is consistent with the greater reaction exothermicity observed when hydrogen is released from CC−AB materials. Scanning electron microscopy shows different morphology of AB in CC−AB nanocomposite as compared to neat AB.

Introduction

Hydrogen storage is a key issue in the developing field of hydrogen technology. Among the chemical hydrides, ammonia borane (AB), also known as borazane or by formula NH_3BH_3, has been of great interest as a hydrogen storage material.[1,2] At ambient temperature and pressure, AB is a stable, white, crystalline solid which contains 19.6% hydrogen by weight.[3] The stages and intermediates of AB dehydrogenation have been studied, and possible pathways have been reported.[4,5] The low-temperature release of hydrogen from solid AB proceeds through two sequential steps.[6] The first equivalent of hydrogen desorbs between 100 and 120 °C (depending on heating rate)[7] to yield polyaminoborane $(BH_2NH_2)_x$. The reaction is moderately exothermic ($\Delta H = -21$ kJ/mol).[8] Continued heating to 150 °C releases a second equivalent of hydrogen to yield polyiminoborane $(BHNH)_x$ and trace quantities of borazine $(B_3N_3H_6)$.[9,10] Borazine is highly volatile and will necessitate strategies to remove this impurity from the hydrogen stream to prevent poisoning of the fuel cell.

For the practical application of AB as a hydrogen storage material for a polymer electrolyte membrane (PEM) fuel cell, the optimum decomposition temperature should be around 85 °C, which is the working temperature of the PEM. Different methods, including catalysts[11] and nanoscale agents,[12] have been used to improve the kinetics of AB dehydrogenation reactions and lower its decomposition temperature. In nanoscale materials, shorter diffusion distances can result in faster kinetics. In addition, changes in surface energies with decreasing particle size can change the thermodynamic stability of the reactants and alter the hydrogen release mechanisms.[13] Infusing AB in mesoporous silica significantly improved the dehydrogenation kinetics and also suppressed borazine formation.[12] However, silica is relatively heavy and has poor thermal conductivity. Alternatively, a similar porous material, carbon cryogel (CC), is lighter, has a tunable pore diameter, and can provide a thermal conduction pathway.[14] The CCs are prepared by sol−gel polycondensation of resorcinol−formaldehyde in aqueous solution.[15] The precursor hydrogels are dried to make aerogels (supercritically dried), cryogels (freeze-dried), and xerogels (vacuum or hot-air-dried). Freeze-drying is an alternative to the expensive supercritical drying method that produces similar porous structure.[16,17] The dried gels are then pyrolyzed to make CCs. We recently reported dehydrogenation for a coherent CC−AB nanocomposite[18] using differential scanning calorimetry coupled with mass spectroscopy. The porous CC like the mesoporous silica showed enhanced rates of hydrogen desorption, up to 9 wt % hydrogen, (1.5 H_2 equiv), at temperatures as low as 90 °C as well as suppressed yields of borazine. On the other hand we observed the opposite for the enthalpy of hydrogen release; instead of a decrease in the reaction exothermicity for hydrogen release as observed in the mesoporous silica (−1 kJ/mol), we observed a significant *increase* in the reaction exothermicity (−120 kJ/mol) for which we had no satisfactory explanation. Here, we follow up with results from spectroscopic studies used to gain some insight into the differences between the porous silica and porous carbon supports. We report new findings from Fourier transform infrared spectroscopy (FTIR) and in situ ^{11}B nuclear magnetic resonance (NMR) results on the dehydrogenation pathways of CC−AB. This information identifies an alternate competing pathway for H_2 release from CC−AB that is consistent with the enhanced kinetics and greater reaction exothermicity relative to neat AB and AB supported on mesoporous silica.

Experimental Methods

Carbon cryogels were derived from resorcinol−formaldehyde hydrogels[16,19] by freeze-drying and pyrolyzing at 1050 °C for 4 h in N_2.[20] The ratio of resorcinol to water was 0.035 g/mL,

* Corresponding authors. E-mail: tom.autrey@pnl.gov and gzcao@u.washington.edu.
[†] University of Washington.
[‡] Pacific Northwest National Laboratory.

10.1021/jp077057t CCC: $37.00
Published on Web 12/04/2007

and the molar ratio of resorcinol to formaldehyde was 0.5. Sodium carbonate was added as a catalyst at room temperature. The resorcinol to catalyst ratio was held at 200:1. The CCs were loaded with AB (BH_3NH_3, Aldrich, tech. 95%) by soaking the cryogels in a solution of 10 wt % AB in tetrahydrofuran (THF) (99.9%, Sigma-Aldrich), under argon at room temperature. After 3−5 h, the solvent was removed under vacuum. Sample weight gain after loading was 40 wt %. The CC−ABs were stored in liquid nitrogen before further analyses.

The pore structure of the CC samples was analyzed by nitrogen physisorption (BET technique) at −196 °C. The multipoint BET and BJH adsorption methods gave a total surface area of 500 m^2/g, a BJH cumulative adsorption surface area of 300 m^2/g, a pore volume of 0.70 cm^3/g, and a pore diameter ranging from 2 to 20 nm with a maximum peak at 5 nm. X-ray photoelectron spectroscopy experiments showed that the carbon and oxygen contents of CC sample were about 96 wt % and 4 wt %, respectively.

Sample morphology was studied by scanning electron microscopy (SEM, Joel JSM-5510LV). Fourier transform infrared spectra were acquired at room temperature using a Nicolet DXB FTIR spectrometer at a resolution of 4 cm^{-1}. The samples for the FTIR were prepared by adding 1 mg of crushed cryogel to 200 mg of dry spectroscopic-grade KBr. The powders were mixed in a mortar and pestle and pressed into a pellet for analysis. Pellets of 2 mg of CC−AB in 200 mg of KBr were also tried but were too opaque.

Thermal decomposition was monitored by isothermal in situ ^{11}B NMR at 18.8 T (800 MHz ^1H frequency). A 4 mm, three-channel, variable temperature Doty probe and a Varian Unity+ console were used. Bloch decay experiments were run using a 4 μs 90° pulse, ∼40 kHz decoupling, and a 10 s pulse delay. A 14 kHz sample spinning was achieved with dry nitrogen gas. The temperature was calibrated by following the chemical shift of ^{207}Pb in $Pb(NO_3)_2$ as a function of temperature.[21] Spectra of ^{11}B were referenced to $NaBH_4$ (−41 ppm).

Results and Discussion

Figure 1 depicts cross-sectional SEM micrographs of cryogels, showing their microstructure before and after loading with AB and also after heating to 150 °C. The porous structure of CC is shown in Figure 1a. Soaking CC in an AB−THF solution results in distribution of AB within the interconnected CC network, which coats the CC scaffold as can be seen in Figure 1b. The AB layer in CC−AB shows a more dense morphology as compared to the foamlike appearance of neat AB.[11] After the dehydrogenation process, the porous structure of CC is sustained and fiber-like residue of AB is scattered throughout the CC (Figure 1c).

To study the decomposition pathways leading to hydrogen release from CC−AB, in situ ^{11}B NMR at 18.8 T was performed. Figure 2 shows the ^{11}B NMR spectra of AB and CC−AB taken at room temperature (left) and taken after heating at 85 °C (right). Upon heating to 85 °C, no change was observed for neat AB (−23.6 ppm) until 35 min. As the transition began, a small side peak was visible at −22.1 ppm, which was attributed to a new phase AB.[9,22] This peak gradually increased, and at the same time, the reaction byproducts (BH_2 peaks at −12 ppm and BH_4 peaks at −38 ppm) are evident. The 50 min time slice is shown in Figure 2b (top).

The major peak observed in the CC−AB before heating has a resonance with a chemical shift of −22.9 ppm, intermediate between new phase AB and neat AB, and may be consistent with the interpretation that the resonance in CC−AB is new

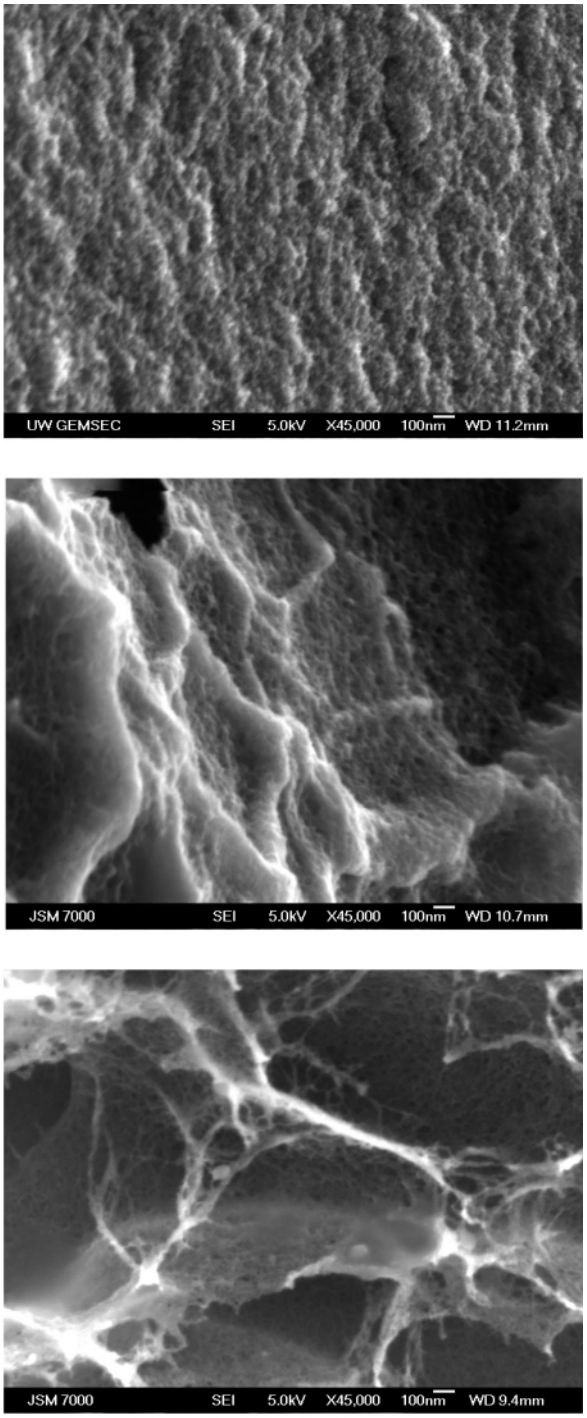

Figure 1. SEM of (a) CC, (b) CC−AB, and (c) thermally reacted CC−AB (heated to 150 °C at 5 °C/min).

phase (for AB scaffolded into mesoporous silica, a chemical shift of −22.6 ppm was observed for new phase AB[23]). The BH_2 and BH_4 peaks (at −12 and −38 ppm) that appear after 35 min in the thermal reaction of neat AB are observed in CC−AB at room temperature. The presence of decomposition products indicates that dehydrogenation is occurring during the incorporation of AB into the CC matrix at room temperature.

Similar product peaks at shorter reaction times are observed for dehydrogenation of CC−AB at higher temperature. Figure 3 compares the in situ ^{11}B NMR spectra for CC−AB before heating, after heating to 85 °C for 10 min, and after heating at 150 °C for 10 min. At 150 °C, the starting material (−22.6 ppm) is completely consumed in less than 10 min.

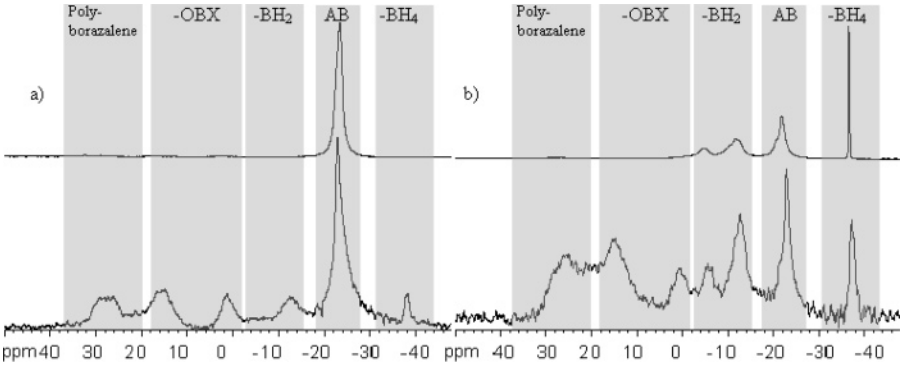

Figure 2. ^{11}B NMR of neat AB (top) and CC−AB (bottom). (a) Before heating. (b) After heating CC−AB for 10 min at 85 °C and AB for 50 min at 85 °C. No reaction of AB at 10 min; data not shown.

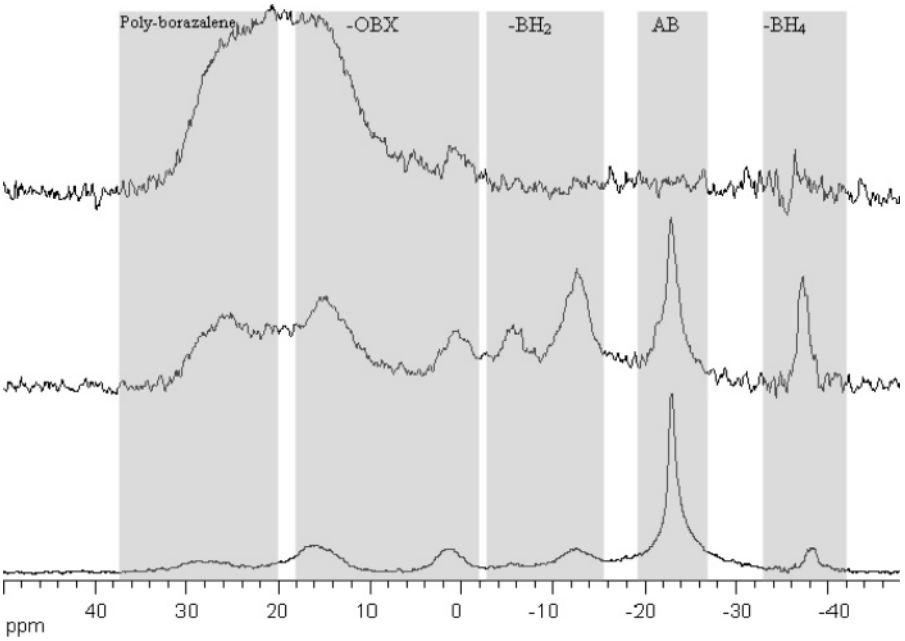

Figure 3. ^{11}B NMR of CC−AB before heating (bottom), after heating to 85 °C for 10 min (middle), and after heating to 150 °C for 10 min (top).

In all of the spectra for CC−AB in Figures 2 and 3, two broad peaks centered at +16 and +28 ppm were present. The peak at +28 ppm was attributed to polyborazylene-like species and indicated more than 1 equiv of H_2 loss from AB.[24] Observation of polyborazylene in CC−AB may indicate that borazine polymerizes in cryogel cavities faster than it can escape to the gas phase, which would explain the suppression of borazine formation during the CC−AB thermal reaction. The borazine suppression was reported earlier in our mass spectroscopy experiments for hydrogen release of the CC−AB nanocomposites.[18] The peak centered at +16 ppm is a new observation in AB decomposition. The peak at +16 ppm was not observed in the neat decomposition of AB or of AB in mesoporous silica. Organic borates are observed in this region of the ^{11}B NMR spectrum, and this resonance is tentatively assigned as the product produced between the reaction of a surface hydroxyl with the borane decomposition products (surface−O−BX_2). The oxygen content of the CC determined by X-ray photoelectron spectroscopy (see Experimental Methods) is sufficient to support this alternative reaction pathway. Furthermore, the formation of thermodynamically stable B−O bonds in the decomposition of AB in CC is consistent with the excess heat release we previously reported for either neat AB or AB on the SBA-15 mesoporous silica supports. Formation of B−O bonds in the AB decomposition of AB in CC is further supported by the apparent bending and breathing modes of B−O bonds in the IR spectra observed between 700 and 1400 cm^{-1} (vide infra).

The FTIR spectrum was used to follow the changes in the functional groups present on the surfaces of CC and CC−AB before and after dehydrogenation. The CC samples are highly absorbing, and high-resolution spectra were difficult to obtain. However, the qualitative results compare and support the results obtained from the in situ NMR experiments. The FTIR spectrum for bulk AB and CC−AB, before and after dehydrogenation (heated to 150 °C at 5 °C/min in an inert atmosphere), are shown in Figure 4. The corresponding wavenumber range and mode for AB obtained from published data[8] are shown on the spectrum. The peaks related to CC are also present but not labeled in the CC−AB spectra. These peaks include the 3424 cm^{-1} related to surface-bound primary OH groups and 1488 cm^{-1} attributed to C═C.[25] Most of the AB peaks in Figure 4a are also present in the CC−AB spectrum. The CC−AB peaks are not as broad as the AB peaks. The narrower peaks may be due to the reduction in the distribution of vibration for AB infused in the CC matrix. However, Figure 4b shows that after the thermal reaction, the CC−AB product spectrum is significantly different from the solid-state AB product spectrum. These differences strongly suggest different decomposition pathways for dehydrogenation of AB and CC−AB. The low-frequency

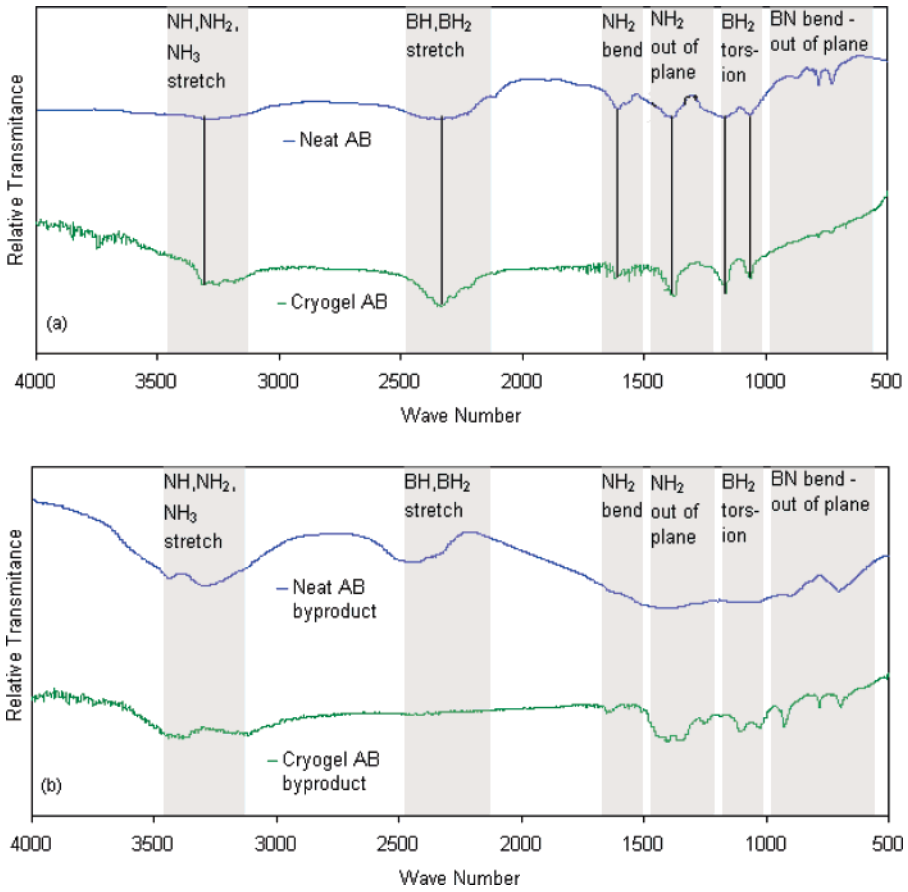

Figure 4. FTIR results for (a) CC−AB and (b) thermally reacted CC−AB (heated to150 °C).

region between 500 and 1500 cm^{-1} and the B−H stretching between 2200 and 2400 cm^{-1} show the greatest changes in the CC−AB and neat AB decomposition products. The three bands at 700, 783, and 930 cm^{-1} in addition to the bands centered near 1400 cm^{-1} are in the region diagnostic of B−O and OBO stretching and bending frequencies.[26] Also, a notable decrease in signal intensity in the B−H stretching region in the CC−AB products is present that would be consistent with the reaction of AB to form alkyl borates in competition with conventional hydrogen loss polyborazylene products observed in the neat AB decomposition.

The results clearly show that dehydrogenation occurs when AB is incorporated in the CC matrix at room temperature and proceeds faster at elevated temperatures when compared to neat AB. The contributing factors to the observed increase in rate, or destabilization of AB, could include the following:

(1) Hydroxyl groups on the surface of CC resulting in the catalysis of the thermolysis of AB.

(2) Defect sites in the CC mesoporous scaffold, possibly in combination with the hydroxyl groups, initiating the reaction at lower temperature.

(3) Limited diffusion of AB provided by the CC mesoporous structure increasing the frequency of interactions, effectively accelerating the dehydrogenation process.

(4) Surface interaction destabilizing the hydrogen-bonding network of neat AB, resulting in a lower barrier to hydrogen release.

The CC support offers enhanced rates of hydrogen release from AB at lower temperatures as observed for the mesoporous silica supports. However, using a lighter carbon support has obvious advantages compared to the heavier silica support. Both materials, CC and SBA-15, contain surface oxygen functionalities, and in both cases surface hydroxyl groups may enhance the kinetics of hydrogen release from AB. One significant difference appears to be a reaction channel available in the CC that leads to products containing B−O bonds resulting in substantially more heat release concurrent with the hydrogen desorption. This was a surprise as formation of B−O bonds between AB and the mesoporous silica, which has a higher density of hydroxyl groups, was not observed.[12] A competing reaction with trace quantities of THF cannot be eliminated. In the IR spectra, THF was not visible, but it is used as the solvent to dissolve and introduce AB into the porous CC. Note, AB does not react thermally with THF in the absence of the CC, so a special reaction channel would need to exist for AB to react with THF that is catalyzed by the presence of CC. Approaches to reduce the surface oxygen content are expected to enhance the stability of AB in carbon supports. Future work includes efforts to control the decomposition of AB at room temperature. Further studies are planned to examine the pore size effects on the kinetics of hydrogen release from CC and aerogel supports.

Conclusions

Using in situ ^{11}B NMR and FTIR experiments to investigate the dehydrogenation of CC−AB nanocomposites, we saw a lower temperature hydrogen release and a new product for CC−AB relative to AB. The new product suggested a new mechanism, namely, the destabilization of AB due to the formation of surface−O−B bonds. Increasing the temperature from 85 to 150 °C did not change the reaction pathways but increased the rate of the dehydrogenation process in the CC−AB nanocomposite. The suppression of borazine, the toxic byproduct in the thermal reaction of neat AB, is also confirmed, providing a promising alternative with fuel cell compatibility.

Acknowledgment. Support for this work is provided by the National Science Foundation (DMR-0605159), WTC, and EnerG2 LLC as well as the U.S. Department of Energy Center of Excellence in Chemical Hydrogen Storage funded by the DOE H_2 Program. Experiments using the FTIR were performed in Professor Zhang's lab in the Materials Science and Engineering Department at the University of Washington. Part of this research was performed in the William R. Wiley Environmental Molecular Sciences Laboratory, a U.S. Department of Energy national scientific user facility located at the Pacific Northwest National Laboratory.

References and Notes

(1) Fakioğlu, E.; Yurum, Y.; Veziroğlu, T. N. *Int. J Hydrogen Energy* **2004**, *29*, 1371.
(2) Seayad, A. M.; Antonelli, D. M. *Adv. Mater.* **2004**, *16*, 765.
(3) Baitalow, F.; Baumann, J.; Wolf, G.; Jaenicke-RoBler, K.; Leitner, G. *Thermochim. Acta* **2002**, *391*, 159.
(4) Baumann, J.; Baitalow, F.; Wolf, G. *Thermochim. Acta* **2005**, *430*, 9.
(5) Stowe, A.; Shaw, W.; Linehan, J.; Schmid, B.; Autrey, T. *Phys. Chem. Chem. Phys.* **2007**, *9*, 1831.
(6) Hoffmann, F. P.; Wolf, G.; Hansen, L. D. *R. Soc. Chem. Cambridge* **1997**, 514.
(7) Hoon, C. F.; Reynhardt, E. C. *J. Phys. C: Solid State Phys*. **1983**, *16*, 6129.
(8) Wolf, G.; Baumann, J.; Baitalow, F.; Hoffmann, F. P. *Thermochim. Acta* **2000**, *343*, 19.
(9) Hu, M. G.; Geanangel, R. A.; Wendlandt, W. W. *Thermochim. Acta* **1978**, *23*, 249.
(10) Sit, V.; Geanangel, R. A.; Wendlandt, W. W. *Thermochim. Acta* **1987**, *113*, 379.
(11) Benedetto, S. D.; Carewska, M.; Cento, C.; Gislon, P.; Pasquali, M.; Scaccia, S.; Prosini, P. P. *Thermochim. Acta* **2006**, *441*, 184.
(12) Gutowska, A.; Li, L.; Shin, Y.; Wang, C. M.; Li, X. S.; Linehan, J. C.; Smith, R. S.; Kay, B. D.; Schmid, B.; Shaw, W.; Gutowski, M.; Autrey, T. *Angew. Chem., Int. Ed*. **2005**, *44*, 3578.
(13) Vajo, J. J.; Olson, G. L. *Scr. Mater.* **2007**, *56*, 829.
(14) Bock, V.; Nilsson, O.; Blumm, J.; Frick, J. *J. Non-Cryst. Solids* **1995**, *185*, 233.
(15) Pekala, R. W.; Alviso, C. T.; Kong, F. M.; Hulsey, S. S. *J. Non-Cryst. Solids* **1992**, *145*, 90.
(16) Tamon, H.; Ishizaka, H.; Yamamoto, T.; Suzuki, T. *Carbon* **1999**, *379*, 2049.
(17) Al-Muhtaseb, S. A.; Ritter, J. A. *Adv. Mater.* **2003**, *15*, 101.
(18) Feaver, A.; Sepehri, S.; Shamberger, P.; Stowe, A.; Autrey, T.; Cao, G. Z. *J. Phys. Chem. B* **2007**, *111*, 7469.
(19) Pekala, R. W. *J. Mater. Sci.* **1989**, *24*, 3221.
(20) Feaver, A.; Cao, G. Z. *Carbon* **2006**, *44*, 590.
(21) Bielecki, A.; Burum, D. P. *J. Magn. Reson., Ser. A* **1995**, *116*, 215.
(22) We have previously observed the narrowing and downfield shift of the ^{11}B resonance of AB in previous studies (ref 5). The appearance of this new peak is believed to be a more mobile phase of AB.
(23) Aardahl, C. U.S. Department of Energy Hydrogen Program. http://www.hydrogen.energy.gov/pdfs/review07/st_28_aardahl.pdf.
(24) Gervais, C.; Framery, E.; Duriez, C.; Maquet, J; Vaultier, M.; Babonneau, F. *J. Eur. Ceram. Soc.* **2005**, *25*, 129.
(25) Hebalkar, N.; Arabale, G.; Vijayamohanan, K.; Ayyub, P.; Kulkarni, S. K. *J. Mater. Sci.* **2005**, *40*, 3777.
(26) Servoss, R. R.; Clark, H. M. *J. Chem. Phys.* **1957**, *26*, 1179.